ISSN 1063-7761, Journal of Experimental and Theoretical Physics, 2016, Vol. 123, No. 6, pp. 991–1007. © Pleiades Publishing, Inc., 2016.
Original Russian Text © A.M. Latyshev, A.V. Bakulin, S.E. Kulkova, Q.M. Hu, R. Yang, 2016, published in Zhurnal Eksperimental'noi i Teoreticheskoi Fiziki, 2016, Vol. 150, No. 6, pp. 1140–1159.

SOLIDS AND LIQUIDS

Adsorption of Oxygen on Low-Index Surfaces of the $TiAl_3$ Alloy

A. M. Latyshev[a], A. V. Bakulin[a,b], S. E. Kulkova[a,b]*, Q. M. Hu[c], and R. Yang[c]

[a] *National Research Tomsk State University, pr. Lenina 36, Tomsk, 634050 Russia*

[b] *Institute of Strength Physics and Materials Science, Siberian Branch, Russian Academy of Sciences, Akademicheskii pr. 2/4, Tomsk, 634055 Russia*

[c] *Shenyang National Laboratory for Materials Science, Institute of Metal Research, Chinese Academy of Sciences, 72 Wenhua Road, Shenyang, 110016 China*

**e-mail: kulkova@ms.tsc.ru*

Received May 2, 2016

Abstract—Method of the projector augmented waves in the plane-wave basis within the generalized-gradient approximation for the exchange-correlation functional has been used to study oxygen adsorption on (001), (100), and (110) low-index surfaces of the $TiAl_3$ alloy. It has been established that the sites that are most energetically preferred for the adsorption of oxygen are hollow (H) positions on the (001) surface and bridge (B) positions on the (110) and (100) surfaces. Structural and electronic factors that define their energy preference have been discussed. Changes in the atomic and electronic structure of subsurface layers that occur as the oxygen concentration increases to three monolayers have been analyzed. It has been shown that the formation of chemical bonds of oxygen with both components of the alloy leads to the appearance of states that are split-off from the bottoms of their valence bands, which is accompanied by the formation of a forbidden gap at the Fermi level and by a weakening of the Ti–Al metallic bonds in the alloy. On the Al-terminated (001) and (110) surfaces, the oxidation of aluminum dominates over that of titanium. On the whole, the binding energy of oxygen on the low-index surfaces with a mixed termination is higher than that at the aluminum-terminated surface. The calculation of the diffusion of oxygen in the $TiAl_3$ alloy has shown that the lowest barriers correspond to the diffusion between tetrahedral positions in the (001) plane; the diffusion of oxygen in the [001] direction occurs through octahedral and tetrahedral positions. An increase in the concentration of aluminum in the alloy favors a reduction in the height of the energy barriers as compared to the corresponding barriers in the γ-TiAl alloy.

DOI: 10.1134/S1063776116110133

1. INTRODUCTION

Among the large number of known intermetallic alloys, the greatest attention of both experimenters and theorists is paid to the alloys based on titanium and aluminum. The titanium aluminides are considered as promising structural materials for the high-temperature applications in the modern branches of industry, such as aerospace, automobile, ship building, etc. These materials possess a whole complex of good mechanical properties, such as low density, high melting point, plasticity, high strength, and heat resistance [1, 2]. The high specific strength and elasticity modulus of Ti–Al compounds as compared to the nickel superalloys make the titanium aluminides very promising for the production of components of contemporary aircraft engines and turbines; however, their corrosion resistance remains less than desired. Furthermore, the balance between the mechanical properties of titanium aluminides and their stability with respect to external factors by no means always can be achieved. For example, the $TiAl_3$ alloy is characterized by a high melting point (near 1340°C), Young's modulus (216 GPa) of the same order as in the nickel-based superalloys, a comparatively low density (about 3.3 g/cm^3) [1, 2], and possesses high corrosion resistance; however, because of the low symmetry of its lattice, this alloy is a rather brittle material. Therefore, the principal goal of the development of new materials based on titanium aluminides is to obtain materials, whose mechanical properties would combine the properties of Ni-based superalloys and of high-temperature ceramics.

The basic problem in the case of the Ti–Al alloys remains an increase in the maximum temperature at which the articles made of these alloys would preserve the necessary mechanical properties. In this context, it is required to deeper understand the process of oxidation of the surface of these alloys depending on their

composition and also to establish factors that can increase their corrosion resistance at high temperatures. The processes of oxidation of both pure titanium and its aluminides have been studied sufficiently well by experimental methods [1, 2]. It is known that oxygen, when interacting with titanium, forms an oxide scale with a rutile structure; the outer oxide layer usually has a columnar structure, which becomes less pronounced with an increase in the temperature; and the inner oxide layer is characterized by a finer structure with equiaxed grains [1–5]. It is assumed that this compact inner oxide layer is an efficient barrier for the diffusion of oxygen. The mechanism responsible for the formation of this layer is connected with stresses that act in the oxide and, consequently, with the creep rate of rutile under oxidation conditions. The transport of oxygen can be substantially affected by the presence of vacancies and defects. The dissolution of oxygen in the titanium substrate upon oxidation can be accompanied by its embrittlement. Furthermore, the rate of the oxygen diffusion depends on the structure of titanium and is higher in β-Ti than in α-Ti [6].

The addition of aluminum makes the oxidation process more complex, since aluminum, just as titanium, has an affinity for oxygen and forms a dense oxide with the structure of corundum α-Al_2O_3, whose formation on the aluminum substrate ensures high corrosion resistance. However, the chemical activity of aluminum is reduced in Ti–Al alloys that contain less than 50% aluminum [1, 7, 8]; this, in combination with the thermodynamic characteristics of the oxides, leads to a larger stability of the interfaces with TiO and TiO_2 than with Al_2O_3. In this connection, it is assumed that on the surface of such alloys there occurs a process of alternating growth of layers with the predominant content, first, of the titanium oxide and, then, of the aluminum oxide. In this case, cracking and partial shedding of the outer layers of the films that do not contact with the alloy can occur [1, 6, 9]. Available experimental data [10–14] show that, at high temperatures, the low corrosion resistance of the titanium aluminides with the aluminum content of 50% and less is caused by the formation of precisely such mixed layers of oxides of titanium and aluminum. The thickness of the external layer of TiO_2 is on the order of several tens of micrometers, and the kinetics of oxidation can be described by a parabolic or even linear law, depending on the temperature of oxidation [14]. At the same time, the examination of the high-temperature oxidation of the $TiAl_3$ alloy in an oxygen atmosphere [14, 15] has shown that in the range of temperatures from 700 to 1200°C there is formed an outer protective oxide layer that almost completely consists of α-Al_2O_3 and controls the kinetics of oxidation. The oxide thickness does not exceed several micrometers; nevertheless, even such a thin layer of Al_2O_3 leads to a substantially lower rate of oxidation of the alloy as a result of the suppression of the oxygen diffusion. According to [14], the low content of titanium in this oxide layer leads to the suppression of nucleation of the TiO_2 phase and, as a result, to the absence of pores and cracks. The anomalously high rate of oxide growth at the initial stage of oxidation of the surface of $TiAl_3$ alloy at temperatures below 1000°C observed in [15] was connected with the internal oxidation of the alloy. The majority of experimental works, for example, [16–20] were devoted to the study of the influence of a third component in the $TiAl_3$ alloy on its corrosion resistance. In particular, it was established that the introduction of Cr, Fe, Ni, and Ag led to improvement in the corrosion resistance of the alloy; in this case, no internal oxidation and formation of the oxides of these elements were observed. At the same time, an impurity of manganese negatively affects the corrosion resistance of the alloy, since it significantly increases the rate of oxidation at temperatures above 1000°C because of the formation of Al_2O_3 with inclusions of TiO_2 particles, although at low temperatures the addition of Mn does not exert such an effect. The admixture of copper favors the formation of TiO_2 and CuO oxides along with Al_2O_3, thus reducing the corrosion resistance of the alloy. Therefore, it follows from the above-mentioned experimental works and references therein that the growth of oxide films directly depends on the composition of surface layers and existing defects. Both the composition of the surface layers and the mechanism of their oxidation can also be substantially affected by the surface segregation of alloy components.

Note that the mechanical and electronic properties of Ti–Al intermetallic compounds have been studied repeatedly by theoretical methods within the framework of the density functional theory (DFT). For example, the authors of [21] have calculated the energies of substitutional defects in the different sublattices of Ti–Al alloys. The effect of impurities on their elastic properties and electronic structure has been studied in [22, 23]. The authors of [24–32] have studied the atomic and electronic structures of the surfaces of titanium aluminides and the adsorption of oxygen on the differently oriented surfaces of alloys. In this respect, the most thoroughly studied alloy is γ-TiAl [24–26, 29–33]. The adsorption of oxygen on the surface of TiAl(111) was studied in [24–26, 30]. It was shown that the most preferred sites of oxygen adsorption on the TiAl(111) surface were Ti-rich positions [24] and that the formation of new Ti–O and Al–O bonds led to the weakening of metallic bonds [25, 26]. The authors of [30–33] studied the adsorption of oxygen on other low-index surfaces of this alloy. In [26, 31], the effects of surface segregation on the processes of oxidation of the TiAl surface were studied. Specific features of the formation of oxide layers on the stoichiometric TiAl(100) surface with the oxygen concentration increasing up to two monolayers (MLs) were examined in our recent work [32]. In addition, we have

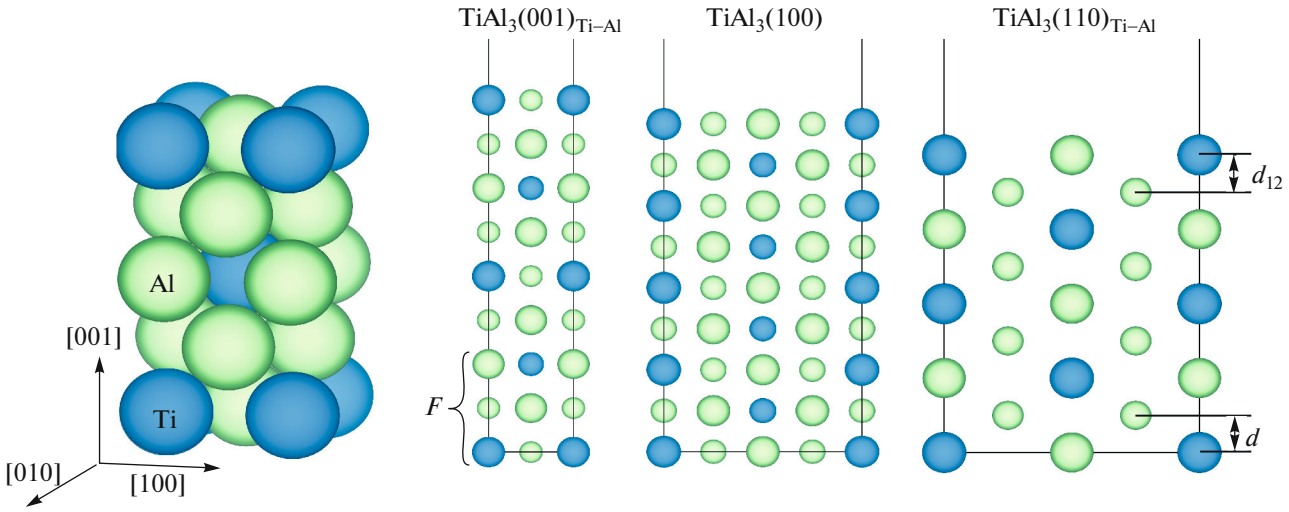

Fig. 1. (Color online) Atomic structure of the $TiAl_3$ alloy (space group $D0_{22}$) and of the (001), (100), and (110) low-index surfaces. Symbol F indicates fixed layers; d and d_{12} are the interlayer spacings in the bulk and on the surface of the alloy.

studied the diffusion of oxygen in the bulk of γ-TiAl alloy and from its surface into the bulk of material [32, 33]. It was established that the sorption of oxygen on the (001), (100), and (110) surfaces, as well as in the bulk of the alloy, was most preferred in Ti-rich positions and that the energy barriers increased upon the diffusion of oxygen from these positions.

The electronic structure of the $TiAl_3$ alloy was also studied in earlier works [34–37]. A considerably smaller attention was paid in the literature to the investigation of the surface structure of this alloy and the interaction of this structure with adsorbed atoms. The surface energy of the $TiAl_3(001)$ surface was calculated in [38], where this surface was modeled by 2- to 8-layer-thick films; however, the adsorption of oxygen on the surface of this alloy was not studied.

Note that the direct simulation of the high-temperature oxidation of the surface of Ti–Al alloys is difficult within the framework of the DFT methods; however, these methods are used intensively in the last decade for studying adsorption and diffusion of interstitial impurities. Although the DFT methods make it possible to obtain information on the ground state of the alloys, it is assumed that for the understanding of the mechanisms of the high-temperature oxidation of the surface of the Ti–Al alloys it is necessary to determine the basic tendencies of the interaction of oxygen with the surface, which are determined by the electron subsystem and practically are independent of temperature. In this connection, it is necessary to conduct comparative and systematic studies of the initial stage of this process, which includes the calculation of the energies of oxygen binding with differently oriented surfaces and the establishment of factors that influence the diffusion of oxygen in the alloys of different composition.

Thus, the purpose of this work is a theoretical study of the oxygen adsorption on the low-index surfaces (001), (100), and (110) of the $TiAl_3$ alloy, as well as of the initial stage of the formation of oxide layers with an increase in the concentration of oxygen on the surface to three monolayers. Another purpose is to reveal the most preferable paths of migration of oxygen atoms in the bulk $TiAl_3$ alloy, which will make it possible to establish the specific features of the oxygen diffusion in the alloy with decreasing content of titanium.

2. METHOD OF CALCULATIONS

The calculation of the atomic and electronic structures of the $TiAl_3$ alloy with the $D0_{22}$-symmetry and of its low-index surfaces (Fig. 1) was carried out by the projector augmented wave (PAW) method in the plane-wave basis [39, 40], which was realized using a VASP program code [41–43], with the generalized gradient approximation for the exchange-correlation functional in the GGA-PBE form [44]. The cut energy of the kinetic energy of plane waves from the basic set was equal to 550 eV. During calculations of the electronic structure of a bulk alloy, the integration over the Brillouin zone was conducted with the use of a $15 \times 15 \times 7$ grid of k points obtained according to the Monkhorst–Pack scheme [45]. The convergence was considered achieved if the difference in the total energies for two successive iterations did not exceed 10^{-5} eV. Note that the theoretical lattice parameters of the alloy ($a = 3.842$ Å and $c = 8.616$ Å) differ from the experimental values ($a = 3.854$ Å and $c = 8.584$ Å [46]) less than by 0.5%.

During simulation of the low dimensionality structures given in Fig. 1, we used the approach of multilayer films separated by a vacuum gap with a thickness of no less than 15 Å. For the $TiAl_3(001)$ surface, we

used a grid of $9 \times 9 \times 1$ k points, whereas for calculating the surfaces with (110) and (100) orientations, grids of $5 \times 9 \times 1$ k points were used. The relaxation of the positions of the atoms of the surface layers (no less than five–six layers, depending on the surface orientation) was conducted with the use of Newton's dynamics until the forces on atoms reached ~0.01 eV/Å.

The calculations of the oxygen adsorption on the low-index surfaces were performed within the framework of the model of asymmetrical films, which was described in detail in our work [32]. Note that oxygen can be adsorbed in different positions on the alloy surface, depending on its orientation. As a rule, there are considered high-symmetry positions in the voids coordinated by three–four surface atoms of the matrix (hollow positions), between two atoms (bridge positions), and over the surface atoms (top positions). The positions of the atoms of three layers on one side of the film were fixed at the values equal to the bulk ones (Fig. 1), and the positions of the atoms of remaining layers were relaxed in three directions. The adsorption energy of an oxygen atom was calculated by the following formula:

$$E_{ads} = -[E_{O-TiAl_3} - E_{TiAl_3} - \frac{1}{2}E_{O_2}], \quad (1)$$

where E_{O-TiAl_3} and E_{TiAl_3} are the total energies of the surface with oxygen and without oxygen, and E_{O_2} is the total energy of an oxygen molecule (9.86 eV). Since in the spin-polarized calculation the binding energy of the oxygen molecule exceeds the experimental value (5.12 eV [48]) by approximately 1 eV [32, 47], in order to compensate for the inaccuracy of the calculations within the DFT, we used the experimental value of the binding energy in the estimations of the adsorption energy of oxygen. The bond length in the oxygen molecule is equal to 1.23 Å, and the energy of an oxygen atom calculated in the cell with dimensions of 12 Å × 12 Å × 12 Å is 1.56 eV.

The estimation of the energy barriers for the diffusion of oxygen atom in the $TiAl_3$ alloy was performed by the method proposed in [49, 50]. In the computational cell, initial and final positions of the oxygen atom were specified along the direction of migration, and five intermediate positions were calculated by the method of linear interpolation. All calculated configurations of the oxygen atom along one direction were relaxed simultaneously; i.e., for each of them the optimum position of the oxygen atom and of the nearest atoms of the alloy, which ensured the minimum values of the energies of all configurations, were determined. The diffusion barrier was estimated as the difference between the energies of the alloy with oxygen in the initial position and at the saddle point.

3. RESULTS AND DISCUSSION

3.1. Energy Stability of Low-Index $TiAl_3$ Surfaces

Let us consider, first, the energy stability of the surfaces of the $TiAl_3$ alloy. As can be seen from Fig. 1, this alloy consists of aluminum and mixed titanium + aluminum layers that alternate along the direction [001]; therefore, the (001) surface has two terminations. Analogously, the (110) surface can be terminated by a layer of aluminum atoms or by a mixed layer, whereas the (100) surface has a stoichiometric composition and is terminated by the mixed layer.

The surface energy was calculated via the following formula:

$$\sigma = \frac{1}{2S}[E_{tot}^{slab} - N_{Ti}\mu_{TiAl_3} - \mu_{Al}^{bulk}(N_{Al} - 3N_{Ti}) - \Delta\mu_{Al}(N_{Al} - 3N_{Ti})], \quad (2)$$

where N_{Ti} and N_{Al} are the numbers of atoms of titanium and aluminum in the film; μ_{TiAl_3} is the chemical potential of the bulk alloy; and $\Delta\mu_{Al}$ is the deviation of the value of the chemical potential of aluminum on the surface of $TiAl_3$ from its value in the bulk aluminum. Since formula (2) was derived as was described earlier in [32], its derivation is not given here. Note that $\Delta\mu_{Al}$ varies in the interval of $-(1/3)\Delta H \le \Delta\mu_{Al} \le 0$, where ΔH is the enthalpy of formation of $TiAl_3$ per formula unit (1.598 eV). The obtained value of ΔH agrees well with the experimental values 1.48–1.59 eV [51, 52]. The test calculations showed that an increase of the number of layers in the film to more than 11 does not lead to substantial changes in the surface energy, and the error in the value of the surface energy is no more than 0.005 J/m^2. A more detailed description of the approach and of the details of the calculation is given in [32].

As can be seen from Fig. 2, the $TiAl_3(110)_{Al}$ surface (hereinafter, the subscript indicates type of the atomic layer by which the surface in question is terminated) is stable almost in the entire permitted range of variation of $\Delta\mu_{Al}$. In the limit of the high concentrations of aluminum, the stable surface is $TiAl_3(001)_{Al}$, although its surface energy is less by only 0.01 J/m^2 than that of $TiAl_3(110)_{Al}$, which is close to the limit of the accuracy of calculations. On the whole, the diagram of the stability of the low-index surfaces of the $TiAl_3$ alloy is similar to the diagram obtained earlier for γ-TiAl [32]. However, there is observed a reduction in the surface energy of mixed terminations $(001)_{Ti-Al}$ and $(110)_{Ti-Al}$ as compared to the titanium terminations of the surfaces of the γ-TiAl alloy with the same orientation. Furthermore, the stoichiometric $TiAl_3(100)$ surface, contrary to TiAl(100), is not stable at any values of the chemical potential of aluminum; however, its surface energy is close to the value for that for (001) in the Ti-rich region. The surface energies of both terminations of the (001) surface are in fact equal (1.80 J/m^2) and

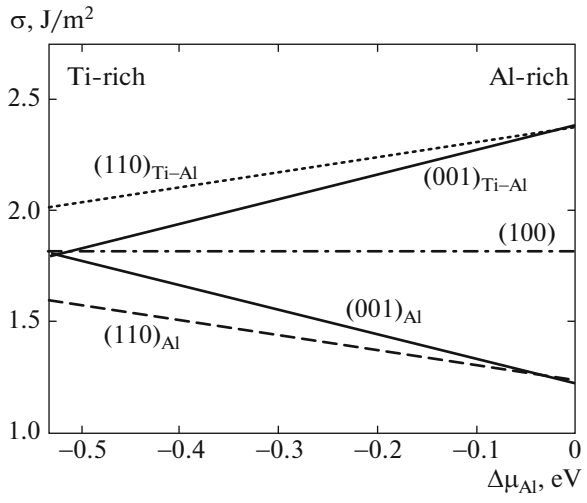

Fig. 2. The diagram of the stability of the low-index surfaces of the $TiAl_3$ alloy.

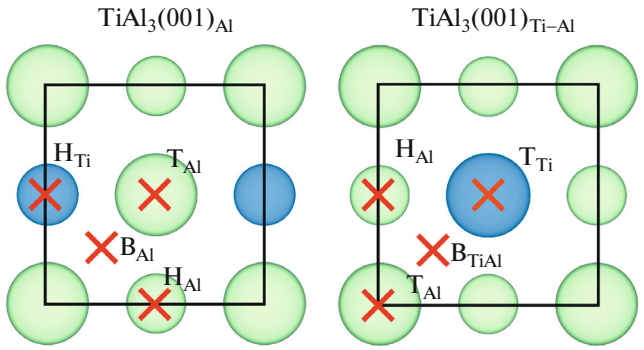

Fig. 3. (Color online) Positions of the oxygen adsorption on two terminations of the nonstoichiometric $TiAl_3(001)$ surface. The large and small blue and light-green balls correspond to the titanium and aluminum atoms of the surface and subsurface layers, respectively.

are in satisfactory agreement with the values of 1.85 and 1.73 J/m^2 obtained in [38] for the six-layer and eight-layer films.

3.2. Adsorption of Oxygen on Low-Index Surfaces of the $TiAl_3$ Alloy

3.2.1. (001) surface. It is known that on the surfaces of metallic compounds the adsorption of oxygen atoms is, as a rule, studied in the case of highly symmetrical positions. On the $TiAl_3(001)$ surface, these are hollow (H), bridge (B), and top (T) positions, which are distinguished by the coordination of the adatom of oxygen (Fig. 3). It follows from Table 1 that, irrespective of the termination of the (001) surface, the most preferable site for the adsorption of oxygen is the hollow position over the aluminum atom of the subsurface layer (H_{Al}). From the bridge B_{Al} position between two aluminum atoms of the surface layer on the $TiAl_3(001)_{Al}$ surface, the oxygen atom is displaced into a more energetically favorable H_{Al} position, which is caused by the presence of two different atoms in the subsurface layer near the B_{Al} position (Fig. 3). The smallest adsorption energy of oxygen is obtained in the case of the top T_{Al} position. The same tendency, namely, the smaller preference of top positions for the adsorption of oxygen, was found for both terminations of the TiAl(001) surface [32]. According to our results obtained for the $Ti_3Al(0001)$ surface, the adsorption energy of oxygen is also higher in the position over the subsurface atom of aluminum than over the titanium atom.

The adsorption energy in the H_{Al} position on the mixed termination of the $TiAl_3(001)_{Ti–Al}$ surface is only 0.11 eV higher than in the bridge B_{TiAl} position between the surface atoms of titanium and aluminum. Oxygen is not displaced from the B_{TiAl} position to H_{Al}, since in this case in the subsurface layer there are located atoms of only aluminum. At the same time, the composition of the surface layer only insignificantly influences the binding energy of oxygen in the H_{Al} position (the difference in E_{ads} for the two terminations is about 0.09 eV); however, the appearance of titanium in the surface layer leads to an increase in the binding energy of oxygen with the surface irrespective of the position of the adsorbate. A similar tendency was obtained earlier for γ-TiAl(001) [32]: the binding energies of oxygen for the titanium termination of the surface are higher than for the aluminum termination. Note also that a twofold increase of the surface computational cell (001) in the lateral directions does not affect the revealed tendencies; the adsorption energy of oxygen changes approximately by 0.1 eV.

It is necessary to say several words about the influence of the oxygen adsorption on the atomic structure of the surface. As a result of splitting of the mixed surface layer of $TiAl_3(001)_{Ti–Al}$ or of the subsurface layer of $TiAl_3(001)_{Al}$, the interlayer spacing between the atoms of surface layers in the case of clean surface changes differently (Table 2). Since the titanium atoms of the subsurface mixed layer are moved toward

Table 1. Adsorption energy (E_{ads}) of oxygen on the $TiAl_3(001)$ surface, positions of oxygen (h_0) relative to the surface layer, and distances between the oxygen atom and nearest atoms of the substrate d(O–M)

Surface	$TiAl_3(001)_{Al}$			$TiAl_3(001)_{Ti–Al}$			
O positions	H_{Al}	H_{Ti}	T_{Al}	H_{Al}	B_{TiAl}	T_{Al}	T_{Ti}
E_{ads}, eV	4.62	3.79	2.20	4.71	4.60	2.87	3.78
h_0, Å	0.87	0.57	1.41	0.79	1.21	1.21	1.67
d(O–Ti), Å	3.90	2.69	4.03	2.09	1.85	2.97	1.71
d(O–Al), Å	2.11	2.00	1.69	2.08	1.81	1.70	3.19

Table 2. Relaxation (in %) of the first interlayer spacing for the clean $TiAl_3(001)$ surface and for the surface with oxygen in the H_{Al} position, and the splitting of the mixed layer. In the parentheses, the values for the atom of aluminum of the second layer over which oxygen is not adsorbed are given

Surface	$TiAl_3(001)_{Al}$			$TiAl_3(001)_{Ti-Al}$		
Parameter	$\Delta d_Z(Al_1-Al_2)$	$\Delta d_Z(Al_1-Ti_2)$	ε_2, Å	$\Delta d_Z(Al_1-Al_2)$	$\Delta d_Z(Al_1-Ti_2)$	ε_1, Å
(001)	−1.5	−7.1	0.12	+2.9	−3.1	0.13
O in position H_{Al} on (001)	+0.17	−10.8	0.24	+8.4 (+1.4)	+7.0 (+0.0)	0.03

the surface in the case of $TiAl_3(001)_{Al}$, this leads to a larger relaxation of the $d_Z(Al_1-Ti_2)$ distance. The splitting in the surface layer of $TiAl_3(001)_{Ti-Al}$ is only 0.01 Å greater than that for the subsurface layer of $TiAl_3(001)_{Al}$. The average value of the relaxation of the surface with the mixed termination does not exceed 0.1%, which agrees well with the result of [38] obtained for an eight-layer film with the application of ultrasoft pseudopotentials. It follows from Table 2 that the adsorption of oxygen in the H_{Al} position on the mixed termination of the $TiAl_3(001)$ surface leads to an increase in the first interlayer spacing. The distance between the subsurface atom of aluminum over which there is no oxygen atom and the surface aluminum atom of the mixed layer also increases, which reflects the indirect interaction of oxygen with the subsurface atoms. At the same time, upon the adsorption of oxygen in the H_{Al} position on the $TiAl_3(001)_{Al}$ surface the negative relaxation $d_Z(Al_1-Ti_2)$ increases, since the titanium atom of the subsurface layer is displaced toward the surface even more strongly. In this case, the splitting of the subsurface mixed layer increases, whereas the splitting of the surface mixed layer in fact disappears upon the adsorption of oxygen on $TiAl_3(001)_{Ti-Al}$ (Table 2).

Since oxygen interacts mainly with the atoms of the surface layer, the changes in the local electron density of states (DOS) of the alloy components are expressed more strongly in the case of $TiAl_3(001)_{Ti-Al}$ (Fig. 4). The interaction of oxygen with the atoms of aluminum of the subsurface layer is not direct but rather is a consequence of the hybridization of 3*s* and 3*p* orbitals of aluminum with the corresponding orbitals of surface atoms. This leads only to inessential changes in the local DOS of the subsurface atoms of aluminum, which can clearly be seen in the lower panels in Fig. 4. On the contrary, the local DOS of the surface atoms of aluminum upon the interaction with oxygen in these positions (Figs. 4a–4c) change to a larger degree than the DOS of the surface atoms of titanium, except for the T_{Ti} position, in which oxygen is adsorbed directly over the surface atom of titanium (Fig. 4d). It is known that the states of the atoms involved in the interaction with oxygen are displaced in comparison with the states for the clean surface. In this connection, the delocalized *s* and *p* orbitals of aluminum more easily form the bonds with *s* and *p* orbitals of oxygen than the more localized *d* orbitals of titanium do. It can be seen from Fig. 4 that the interaction of oxygen with the surface leads to the appearance of peaks in the local DOS curves of the surface atoms of Al and Ti, the positions of which on the energy scale coincide with the peaks of 2*s* and 2*p* bands of oxygen. The calculation of partial DOS of oxygen has shown that its 2*s* band is located at the energies from −16 to −20 eV (depending on the position of the adsorbed atom). In the same region, there are observed small peaks of DOS of the atoms of aluminum and titanium (Figs. 4a, 4b) split-off from the bottom of the valence bands of metals and caused by the hybridization of their states with the 2*s* states of oxygen. The wider 2*p* band of oxygen lies nearer to the Fermi level. The positions of the sharp peaks of the 2*p* bands of oxygen also agree well with the positions of the DOS peaks of aluminum, which are located nearer to the Fermi level at the energies from −6.0 to −3.0 eV (they are shown by arrows in Figs. 4a–4c). These peaks reflect the interaction of 2*p* orbitals of oxygen with the corresponding 3*p* orbitals of aluminum, whereas the peaks located somewhat farther from the Fermi level, for example, at the energies of −8.0 eV (Fig. 4a), −6.3 eV (Fig. 4b), and −4.2 eV (Fig. 4c), are the consequence of the interaction of 2*p* orbitals of oxygen with 3*s* states of aluminum. It is necessary to note that with an increase in the binding energy of oxygen with the surface there occurs a shift of the centers of gravity of both valence *s* and *p* subbands of oxygen toward negative energies. On the whole, the strong hybridization of the *s* and *p* states of oxygen with the orbitals of both surface atoms leads to a larger preference of the hollow H_{Al} and bridge B_{TiAl} positions for the adsorption of oxygen on the mixed termination of the $TiAl_3(001)_{Ti-Al}$ surface. The hybridization of the states of surface atoms with the 2*p* states of oxygen leads to the appearance of low-lying states, which also begin to split-off from the edges of the valence bands of Al and Ti. Since similar tendencies in the changes in the local DOS of surface atoms also occur upon the adsorption of oxygen on $TiAl_3(001)_{Al}$, we will not analyze them here.

It is necessary to note that the smallest energy of binding of oxygen in the top positions is caused by the circumstance that in this case the chemical bond is formed via the interaction of oxygen with the $3p_z$ orbitals of aluminum or with the $3d_{z^2}$ orbitals of titanium;

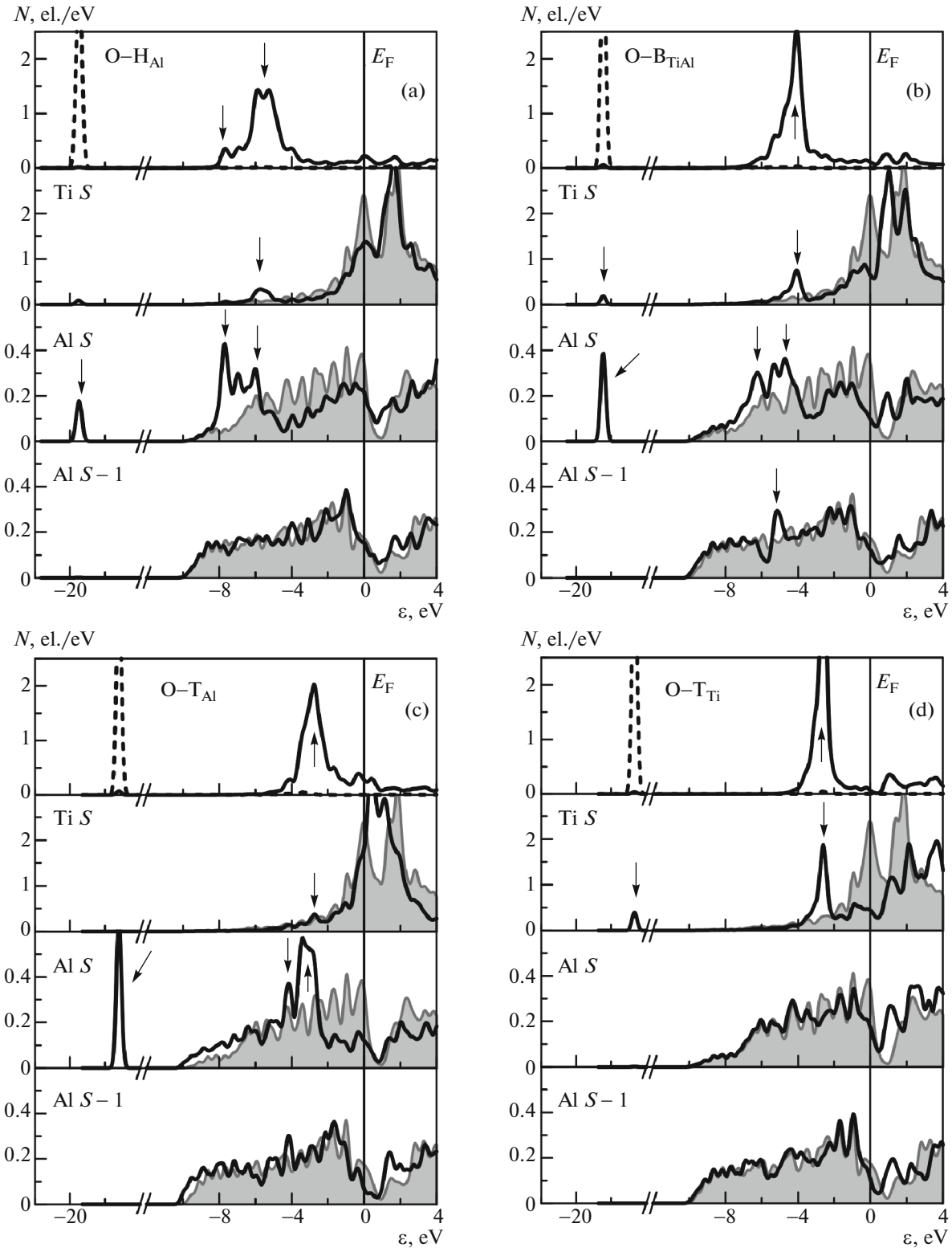

Fig. 4. Densities of electron states of oxygen and of surface (S) and subsurface ($S-1$) Ti and Al atoms depending on the position of oxygen adsorption on the $TiAl_3(001)_{Ti-Al}$ surface. In the upper panels, s and p states of oxygen are shown by dashed and solid curves, respectively. Gray color shows the total DOS corresponding to atoms on a clean surface.

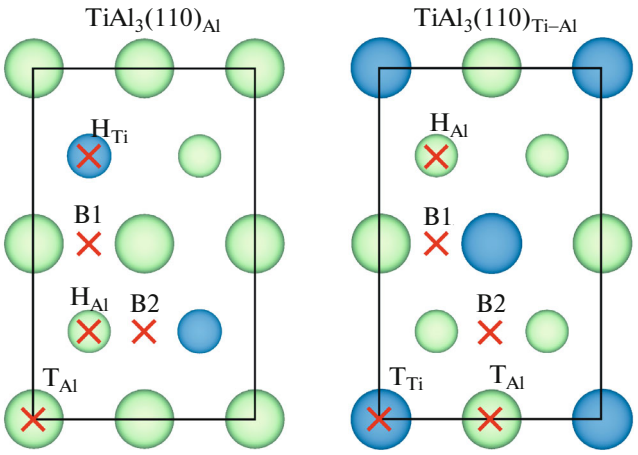

Fig. 5. (Color online) Oxygen adsorption positions on the $TiAl_3(110)$ surface depending on its termination. The designations as in Fig. 3.

however, the latter are almost not filled. In this case, the charge necessary for the interaction with electronegative oxygen can be obtained due to a redistribution of the charge from other filled orbitals of these atoms or from the nearest neighbors. It can be seen that upon the interaction of oxygen in the top positions (Figs. 4c, 4d) there occurs an exhaustion of the states of the corresponding surface atoms. Furthermore, the transfer of a charge from the substrate to the oxygen atom in the top positions (0.75–1.23e) is significantly less than in the case of hollow H positions (1.46–1.97e). Thus, the preference of the hollow positions is caused by the increase of the ionic contribution to the mechanism of the chemical bonding of oxygen with the alloy surface.

3.2.2. (110) surface. The $TiAl_3(110)$ surface, just as (001), also has two possible terminations: aluminum and mixed. The surface cell of (110) is rectangular with the dimensions of 5.433 Å and 8.616 Å. The interlayer spacing in this case is 1.358 Å, which is considerably less than the corresponding spacing (2.154 Å) in the case of the (001) surface. The calculation of the relaxation of the interlayer spacings for both terminations of this surface has shown that there is observed a substantial contraction of the first interlayer spacing and that the relaxation (–14.2%) for $TiAl_3(110)_{Al}$ surface significantly exceeds that (–7.4%) for $TiAl_3(110)_{Ti–Al}$. Note that the values given above were calculated using the average positions of atoms in the mixed layer. The splitting in the mixed layer is equal to 0.154 Å and 0.136 Å for the aluminum and mixed terminations of the (110) surface, respectively; the atoms of aluminum are located higher than the titanium atoms. On the whole, on this surface there is observed an alternating relaxation of the interlayer spacings, which attenuates with moving into the depth of the film more slowly than in the case of the (001) surface.

The adsorption positions of the oxygens on the two terminations of the $TiAl_3(110)$ surface are shown in Fig. 5. Apart from the positions noted above, there are two nonequivalent bridge positions on the (110) surface, which we will call short-bridge (B1) and long-bridge (B2) positions. It follows from Table 3 that, irrespective of the termination of the (110) surface, the largest energy of the oxygen adsorption corresponds to the short-bridge B1 position. Let us briefly discuss the structural and electronic factors that are responsible for the preference of this B1 position for oxygen adsorption on the example of the stable $TiAl_3(110)_{Al}$ surface. It can be seen from Fig. 6a that the oxygen atom is shifted from the B1 position toward the H_{Ti} position and lies approximately at the center of the triangle formed by two surface aluminum atoms and one subsurface titanium atom. In this case, the calculated lengths of the O–Al and O–Ti bonds (Table 3) for the equilibrium configuration are close to the sum of the covalent radii of oxygen and corresponding metals. The difference in the atomic radii of titanium and aluminum (about 0.14 Å) suggests a smaller value of the length of the O–Al bond. The titanium and aluminum atoms involved in the interaction with oxygen in the B1 position are shifted differently relative to the surface layer: the aluminum atom is displaced by 0.1 Å toward the side of vacuum, whereas the titanium atom is displaced insignificantly (by 0.01 Å) into the bulk of the alloy.

The oxygen atom in the long-bridge B2 position is introduced into the subsurface layer to a depth of 0.05 Å (the negative value of h_0 in Table 3 means that the adatom of oxygen is located below the atoms of the surface layer); it introduces even deeper into the subsurface layer on the mixed termination of the surface (Table 3); however, in the B1 position the oxygen atom is located substantially higher than the surface layer. In addition, in the B2 position the oxygen atom is displaced by 0.25 Å toward the H_{Al} position (Fig. 6b), which leads to the formation of its bond with the subsurface atom of aluminum as well (Table 3). At the same time, the distance between the oxygen and surface atoms of aluminum in the B2 position of the $TiAl_3(110)_{Al}$ surface is greater by 0.29 Å than in the B1 position, which indicates a weaker interaction of oxygen with the surface in this position. This is confirmed by the calculations of the DOS of the atoms of surface layers for these two positions (Figs. 6c, 6d). Upon the adsorption of oxygen in the B1 position, there is observed a sharp peak in the DOS of the surface atoms of aluminum at –19 eV, as well as substantial changes in the DOS below –4.0 eV (Fig. 6c). The two-peak structure of the valence 2p band of oxygen is the consequence of a strong hybridization of 2p states of oxygen both with 3s and 3p orbitals of aluminum. The smaller oxygen peak at the energy of –6.5 eV is in agreement with the sharp peak of 3s states of aluminum, whereas the 3p states of aluminum have the same

Table 3. Adsorption energy (E_{ads}) of oxygen on the $TiAl_3(110)$ surface, positions of oxygen (h_0) relative to the surface layer, and distances between the oxygen atom and nearest atoms of the substrate $d(O–M)$

Surface	O position	H_{Al}	H_{Ti}	B1	B2	T_{Al}	T_{Ti}
$TiAl_3(110)_{Al}$	E_{ads}, eV	2.59	2.77	4.87	4.26	1.91	–
	h_0, Å	0.29	0.61	0.59	–0.05	1.68	–
	d(O–Ti), Å	3.19	1.82	2.21*	2.06*	4.01	–
	d(O–Al), Å	2.50, 1.79*	2.63	1.78	2.07, 1.86*	1.68	–
$TiAl_3(110)_{Ti–Al}$	E_{ads}, eV	4.58	–	5.45	4.92	2.95	3.86
	h_0, Å	0.22	–	1.07	–0.25	1.53	1.71
	d(O–Ti), Å	2.05	–	1.83	1.89	3.16	1.71
	d(O–Al), Å	2.78, 1.92*	–	1.77	2.91, 1.91*	1.68	3.28

*Asterisks indicate distances from an oxygen adatom to atoms of the subsurface layer.

two-peak structure as that of the valence band of oxygen in this energy range.

In the B2 position, the oxygen is mainly interacts with more strongly delocalized 3*s* orbitals of surface aluminum. The fine structure of the DOS of aluminum has the same specific features as the DOS of oxygen. As can be seen from Fig. 6d, the positions of the peaks of the *d* states of subsurface titanium atoms and 3*p* states of subsurface aluminum agree well with the sharp peak of the DOS of oxygen at the energy of –5.5 eV. Thus, in the interaction with oxygen there are involved mainly atoms of aluminum of the subsurface layer. However, the greater length of the O–Al bond and smaller (by 0.1*e*) charge transfer than in the B1 position cause a smaller preference of the B2 position for the adsorption of oxygen. Note that the charge transfer to oxygen from the substrate in the case of the B1 position is 1.6*e*. The change in the electronic characteristics on the mixed termination is similar to that described above; therefore, it is not discussed here. On the whole, the appearance of titanium in the surface layer, just as on the (001) surface, increases the energy of oxygen bonding with this surface (Table 3).

3.2.3. (100) surface. The (100) surface is stoichiometric, in contrast to the two above-considered surfaces; i.e., in each atomic layer in the direction [100] there are located three atoms of aluminum and one atom of titanium. The distance between the (100) atomic planes in the $TiAl_3$ alloy is 1.92 Å, which is an intermediate value between the values of the interlayer spacings for the (110) and (001) planes. The average value of the relaxation is –2.6% for the first interlayer spacing; in this case, it is the distances between aluminum atoms that are reduced more strongly. A small positive relaxation (0.6%) was obtained for the second interlayer spacing. The aluminum atoms located in one layer are not equivalent, since they have different coordinations (Fig. 7a). The nonequivalent atoms Al1 and Al2 located in the subsurface layer (Fig. 7a) are displaced during the relaxation differently: the atom Al1 is shifted only in the normal direction, whereas the atom Al2 is also displaced insignificantly in the surface plane. In the surface layer, the displacement of this Al atom is 0.03 Å, and the splitting between the nonequivalent atoms of aluminum in the direction of the normal to the surface is equal to 0.08 Å. However, this splitting decreases for the subsurface atoms of aluminum (about 0.01 Å). Furthermore, the atoms of aluminum located in the centers of the quadrangles formed by two atoms of titanium and two atoms of aluminum are located higher than titanium atoms by 0.02 Å. All these features of the clean $TiAl_3(100)$ surfaces lead to the appearance of a larger number of positions in which an oxygen atom can be adsorbed on this surface (Fig. 7a).

It follows from Table 4 that the highest energy of oxygen adsorption corresponds to the bridge B_{TiAl} position between the surface atoms of Ti and Al. Recall that the bridge positions were found to be preferable for oxygen adsorption also on the (110) surface. Among all the positions considered, the B_{TiAl} position is characterized by the smallest lengths of oxygen bonds with the nearest surface atoms (Table 4), which also indicates the strong chemical binding of oxygen with the surface in this position. At the same time, from the bridge position B_{Al} between the atoms of aluminum, the oxygen atom is displaced into the H_{Al2} position above the aluminum atom of the second layer. This hollow position in the quadrangle formed by one atom of titanium and three atoms of aluminum is most preferable for the adsorption of oxygen among the three possible H positions. The latter is caused by the strong binding of oxygen with the surface titanium atom toward which the oxygen atom is displaced by 0.46 Å. The length of the O–Ti bond in the H_{Al2} position is less by 0.16 Å than the length of the corresponding bond in the H_{Al1} position, which indicates a stronger hybridization of the *s* and *p* orbitals of oxygen with the *s* and *d* orbitals of titanium in the first case. This conclusion is confirmed by the calculations of the local and partial densities of states of the surface atoms for different H positions. The energies of adsorption of

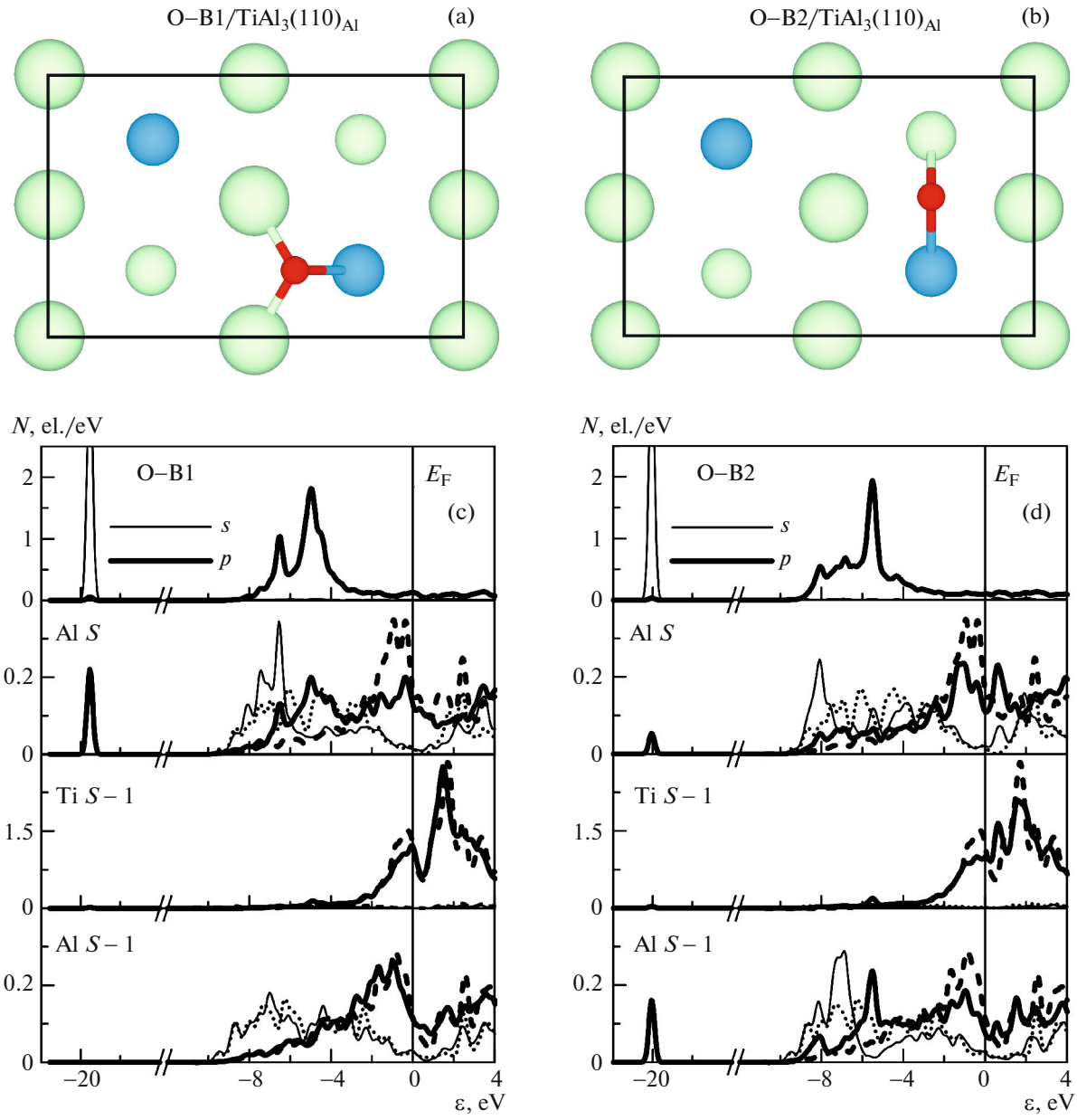

Fig. 6. (Color online) Atomic structures of the $TiAl_3(110)_{Al}$ surface with oxygen adatoms in the positions (a) B1 and (b) B2 (top view) and (c, d) local DOS of oxygen and surface (S) and subsurface ($S-1$) atoms of Al and Ti that correspond to these positions of the adsorbed atoms. The dotted and dashed curves show the DOS of atoms for the clean surface.

oxygen in the T positions above both surface atoms, just as on the (001) and (110) surfaces, are smallest.

On the whole, the changes in the densities of electron states of atoms that are nearest to oxygen depending on the oxygen position on the (100) surface (Figs. 7b, 7c) are similar to those considered earlier for other surfaces. Note that oxygen upon the adsorption in the bridge B_{TiAl} position gives two sharp peaks centered at the energies of –19 and –4.2 eV (Fig. 7b). At the same energies, in the local DOS of titanium and aluminum there are peaks induced by the interaction with oxygen, which are shown by arrows in Fig. 7. It can be seen that the DOS peak of the surface aluminum at the energy of –4.2 eV is mainly caused by 3*p* states, which change more substantially upon the interaction with oxygen than the 3*s* states. The interaction of oxygen with the 3*s* states of aluminum leads only to a broadening of the sharp peak of oxygen and to the appearance of small features in its left arm. At the same time, the states of the subsurface aluminum atom practically do not change, since they are excluded from the direct interaction with oxygen. Upon the adsorption of oxygen in the H_{Al2} position, it is the 3*s* states of aluminum that change to a larger

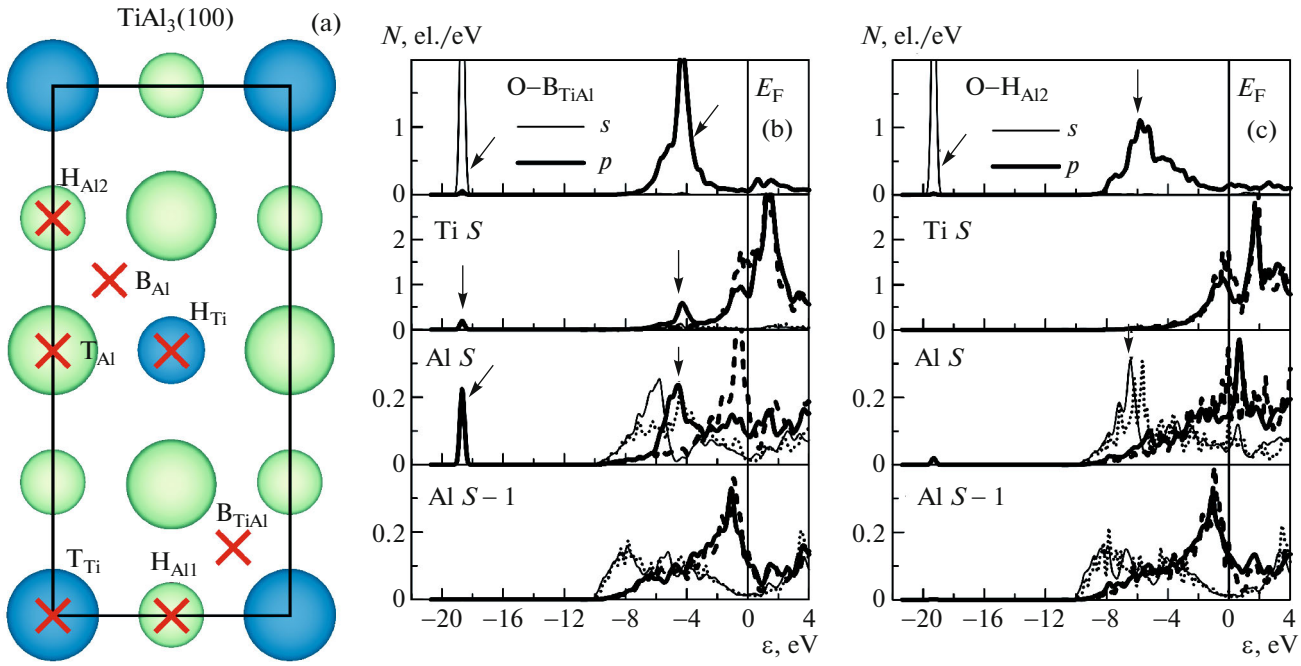

Fig. 7. (Color online) (a) Positions of the oxygen adsorption on the $TiAl_3(100)$ surface and (b, c) partial DOS of oxygen and nearest surface (S) and subsurface ($S-1$) atoms of aluminum and titanium for the positions (b) B_{TiAl} and (c) H_{Al2}. The dashed curves show the DOS of the corresponding atoms for the clean surface.

degree (Fig. 7c), since there is only a small peak caused by the changes in the 3*p* states of aluminum. This leads to the appearance of a two-peak structure of the DOS of oxygen, and the smaller peak at the energy of –5.2 eV reflects the hybridization of the 2*p* states of oxygen with the 3*p* orbitals of aluminum. In this case, the depletion of the 3*d* states of titanium also occurs, which are involved into the interaction with oxygen in this position to a lesser degree than in the case of B_{TiAl}.

In general, the results obtained indicate a decrease in the binding energy of oxygen on the low-index surfaces of the $TiAl_3$ alloy irrespective of the position of adsorption in comparison with TiAl, which is in agreement with the experimental data [53].

3.3. Influence of the Oxygen Concentration on the Atomic and Electronic Properties of the Surface

Let us analyze the influence of the oxygen concentration on the atomic and electronic structures of the $TiAl_3(001)$ surface depending on its termination. We used the approach upon which the additional atoms of oxygen were placed into positions according to the following energy preference. The aluminum termination of the (001) surface is more stable in the limit of the high concentrations of aluminum according to our calculations of the surface energies of low-index surfaces (Fig. 2). In this case, the tendencies in the changes in the density of the electron states of the surface atoms of aluminum remain similar to those that were established earlier for the adsorption of oxygen on the TiAl(100) surface [32]. As was shown above, the adsorption of one atom of oxygen on the Al-rich (001) surface, which corresponds to the degree of coverage equal to 0.5 ML, leads to the formation of states in the DOS of the surface atoms of aluminum, which begin to split off from the bottom of the valence bands (Fig. 8a, the second panel from top) as a result of the formation of new bonds with oxygen. Let us recall that the degree of coverage in this work we defined as the ratio of the number of oxygen adatoms to the number of atoms in the surface layer of the substrate. The electronic structure of subsurface titanium almost does not differ from the appropriate DOS of titanium on the clean surface, since it is located at a distance of 3.90 Å from oxygen and interacts with it through the hybridization with the surface atoms of aluminum rather than directly. It can be seen from Fig. 8a that in

Table 4. Adsorption energy (E_{ads}) of oxygen on the $TiAl_3(100)$ surface, positions of oxygen (h_0) relative to the surface layer, and distances between the oxygen atom and nearest atoms of the substrate $d(O-M)$

O position	H_{Al1}	H_{Al2}	H_{Ti}	B_{TiAl}	T_{Al}	T_{Ti}
E_{ads}, eV	4.28	4.71	4.11	4.99	2.36	3.53
h_0, Å	0.71	0.82	0.30	1.09	1.52	1.69
d(O–Ti), Å	2.06	1.90	2.39	1.85	4.11	1.69
d(O–Al), Å	2.22	2.15	1.96, 2.28	1.79	1.68	3.52

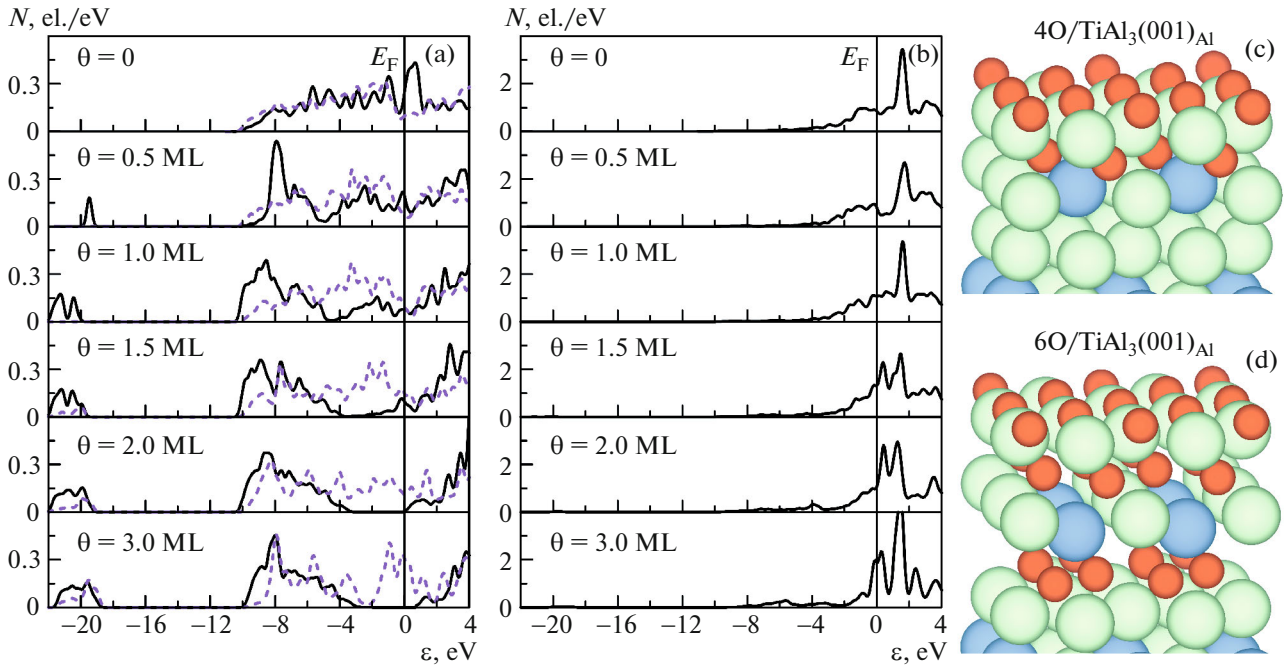

Fig. 8. (Color online) Local DOS of (a) (solid curve) surface and (dashed curve) subsurface atoms of Al and (b) subsurface atoms of Ti that are nearest to oxygen; (c, d) atomic structures for the case of (c) 2.0 ML and (d) 3.0 ML of oxygen on the $TiAl_3(001)_{Al}$ surface.

the local DOS of the surface atoms of aluminum in the region of –4.5 eV there is formed a pseudo-gap, which becomes wider with an increase in the concentration of oxygen and is displaced toward the Fermi level (E_F). At the degree of coverage of oxygen equal to 1.5 ML, when one of the atoms penetrates into the subsurface layer, in the DOS of the subsurface atoms of titanium there also begin to appear split-off states in the region from –8.0 eV to –4.0 eV (Fig. 8b), which reflects the direct interaction of titanium with oxygen. In this case, the interatomic spacing Ti–O is 2.10 Å. Figures 8c and 8d display the variation of the atomic structure of the surface upon high concentrations of oxygen, when the latter penetrates into the subsurface layers, occupying tetrahedral positions. At 2.0 ML of oxygen, the splitting of the mixed layer is 0.12 Å, but it increases to 0.72 Å at 3.0 ML of oxygen. In both cases, the titanium atoms are located below the subsurface atoms of aluminum. In Fig. 8a, it can be seen that the formation of oxide layers on the aluminum termination of the (001) surface practically stops at the degree of coverage with oxygen equal to 2.0 ML. At the same time, in the DOS of the subsurface atoms of titanium (Fig. 8b) even at the degree of coverage with oxygen equal to 3.0 ML there is a high density of electron states at the Fermi level, $N(E_F)$, and the states lying below, at the energies from –8.5 to –2.0 eV, are not completely split-off. The local DOS of the subsurface atom of aluminum also demonstrates the presence of a density of states at the Fermi level. Thus, on the one hand, the states of subsurface atoms are already involved into the interaction with oxygen, but, on the other hand, the metallic Ti–Al bonds still exist. Furthermore, on the $TiAl_3(001)$ surface there is formed a subsurface region enriched by aluminum (Fig. 8d), which contributes to the formation on the surface of the $TiAl_3$ alloy of a protective film of Al_2O_3, which is assumed to be responsible for the high corrosion resistance of the alloy. Similar changes in the atomic and electronic structure were revealed by our calculations of the oxygen adsorption on the $TiAl_3(110)_{Al}$ surface. These results are not discussed in this work, since the tendencies revealed do not differ from those described above.

In our opinion, of more interest is the behavior of oxygen on the mixed termination of the $TiAl_3(001)_{Ti–Al}$ surface, since in this case both components of the alloy are involved into the interaction with oxygen, which manifest itself vividly in the appropriate atomic and electronic characteristics (Fig. 9). With the degree of coverage with oxygen equal to 0.5 ML (Fig. 9a), there are observed changes in the local DOS of surface atoms similar to noted above; namely, there are formed low-lying states near the bottom of the valence bands of Al and Ti (Figs. 9f, 9g), and in the region of –4.0 eV there appears a pseudo-gap, which indicates a change of the mechanism of bonding in the surface layers. The adsorption of a second atom of oxygen in the H_{Al} position (Fig. 9b) leads to a splitting of the mixed surface layer; in this case, the aluminum atoms lie higher by 0.87 Å than the titanium atoms. This suggests that on the surface of the $TiAl_3$ alloy the interac-

tion of oxygen with aluminum is stronger than with titanium. In the DOS of surface atoms, there is observed a further splitting-off of lower-lying states from the bottom of the valence bands of metals; in this case, the pseudo-gap is extended from −4.0 to −2.0 eV. Upon a monolayer coverage with oxygen on the $TiAl_3(001)_{Ti-Al}$ surface, the number of split-off states located at the energies near −19 eV increases, and the states themselves are displaced almost by 1 eV toward the negative energy. This effect is more strongly pronounced in the DOS of the aluminum atom, which indicates a strengthening of the O–Al bonds on the surface. A further increase in the concentration of oxygen favors the penetration of the oxygen atom adsorbed in the H_{Al} position into the subsurface layers (Fig. 9c), where it occupies a tetrahedral position between the surface and subsurface layers. The incorporated atom of oxygen is located lower by 0.99 Å than the titanium atoms of the surface layer, whose splitting decreases to 0.75 Å. The pseudo-gap in the DOS of aluminum is extended almost to E_F, at which there is only a low density of electron states, although $N(E_F)$ remains significant for the titanium states.

At an oxygen concentration of 2.0 ML, the splitting of the surface layer decreases to 0.23 Å; in this case, it is already the titanium atoms that lie higher than the aluminum atoms. Thus, with an increase in the concentration of oxygen its interaction with titanium on the surface is strengthened, which is reflected in the local DOS of titanium (Fig. 9f). In particular, the width of the valence band of titanium increases to 7 eV, and $N(E_F)$ decreases from 2.4 to 1.4 el /eV. The number of states lying below, in the region of −21 eV, which are due to the interaction of the 2*s* orbitals of oxygen with the 4*s* orbitals of surface Ti, also increases. The states split-off at the energies from −10 to −3 eV are mainly caused by the interaction of the *p* orbitals of oxygen with *s* and *d* states of titanium. The appearance of a pseudo-gap in the DOS of titanium or aluminum indicates the formation of new Ti–O and Al–O bonds and a weakening of Ti–Al metallic bonds in the surface layers. At the same time, the presence of states at E_F at the degree of coverage with oxygen equal to 2.0 ML indicates that the metallic nature of the surface is not completely lost. The analysis of atomic structures and of their electronic characteristics indicates that the process of the formation of oxide layers on the surface of the $TiAl_3(001)$ alloy with the mixed surface termination and of new bonds with an ionic nature practically is completed at the degree of coverage with oxygen equal to 3 ML. It can be seen from Fig. 9e that at this concentration the oxygen atoms displace the titanium atoms toward the surface and also are incorporated into the split Ti–Al layer; as a result, the interlayer spacing between the atomic layers of titanium and aluminum increases substantially (to 1.63 Å). This behavior is caused by the larger activity of titanium in the intermetallic alloys. It is known that the energy of self-diffusion of titanium in titanium aluminides is by an order of magnitude higher than that of aluminum [54]. Furthermore, the energy of the formation of titanium oxides is less than that of Al_2O_3 [55]. It can be seen from Fig. 9e that there is formed a layered structure with an outer layer of the titanium oxide and an inner layer of the aluminum oxide. In this case, the subsurface atoms of aluminum are sixfold-coordinated by oxygen; the lengths of the O–Al bonds are 1.92–2.10 Å. The lower atoms of Al have only two bonds with oxygen, whose length is equal to 1.81 Å. Recall that the lengths of Al–O bonds in Al_2O_3 are 1.86–1.97 Å. The bond lengths and the chemical composition of this region indicate the beginning of the formation of Al_2O_3 in the subsurface region.

Thus, the above analysis of the structural and electronic factors has shown that at the low concentrations of oxygen on the mixed termination of the (001) surface a more preferred process is the formation of oxygen bonds with the aluminum atoms, whereas as the oxygen concentration increases, bonds with titanium are formed more easily. As it was noted in [31], the formation of substitutional defects (aluminum at the site of titanium) on the mixed TiAl(100) surface occurs easier than the substitution of titanium for aluminum (0.46 eV and 2.15 eV, respectively). However, the adsorption of oxygen favors the surface segregation of titanium; this leads to the selective oxidation of titanium and the formation of titanium oxides at the initial stage of the surface oxidation [53]. It is precisely such a behavior that can be observed, also, on the mixed termination of the $TiAl_3(001)$ surface. The influence of defects and oxygen on the surface stability of the low-index surfaces of the $TiAl_3$ alloy requires a more detailed study.

On the whole, the investigations conducted demonstrate a strong dependence of the mechanism of oxidation on the composition of surface layers. It is obvious that subsequently a more careful study of the segregation of impurities on the surface of the alloy, as well as of their influence on the adsorption and diffusion of oxygen through the interface should be performed. As was shown in our work [55], impurities such as Zr, Nb, Mo, Hf, Ta, W, and Re increase the energy of the formation of vacancies in TiO_2; therefore, the resulting inner oxide layer can serve as an efficient barrier for oxygen diffusion.

3.4. Diffusion of Oxygen in the Bulk $TiAl_3$ Alloy

In conclusion, let us examine the diffusion of oxygen in the bulk of the $TiAl_3$ alloy and consider the obtained energy barriers with the results for the γ-TiAl alloy of equiatomic composition. Since the dimensions of the lattice in the directions [100] and [010] are two times less than in [001], the minimum size of computational cell for the analysis of the oxygen diffusion is (2 × 2 × 1). As was shown in our work [32], an

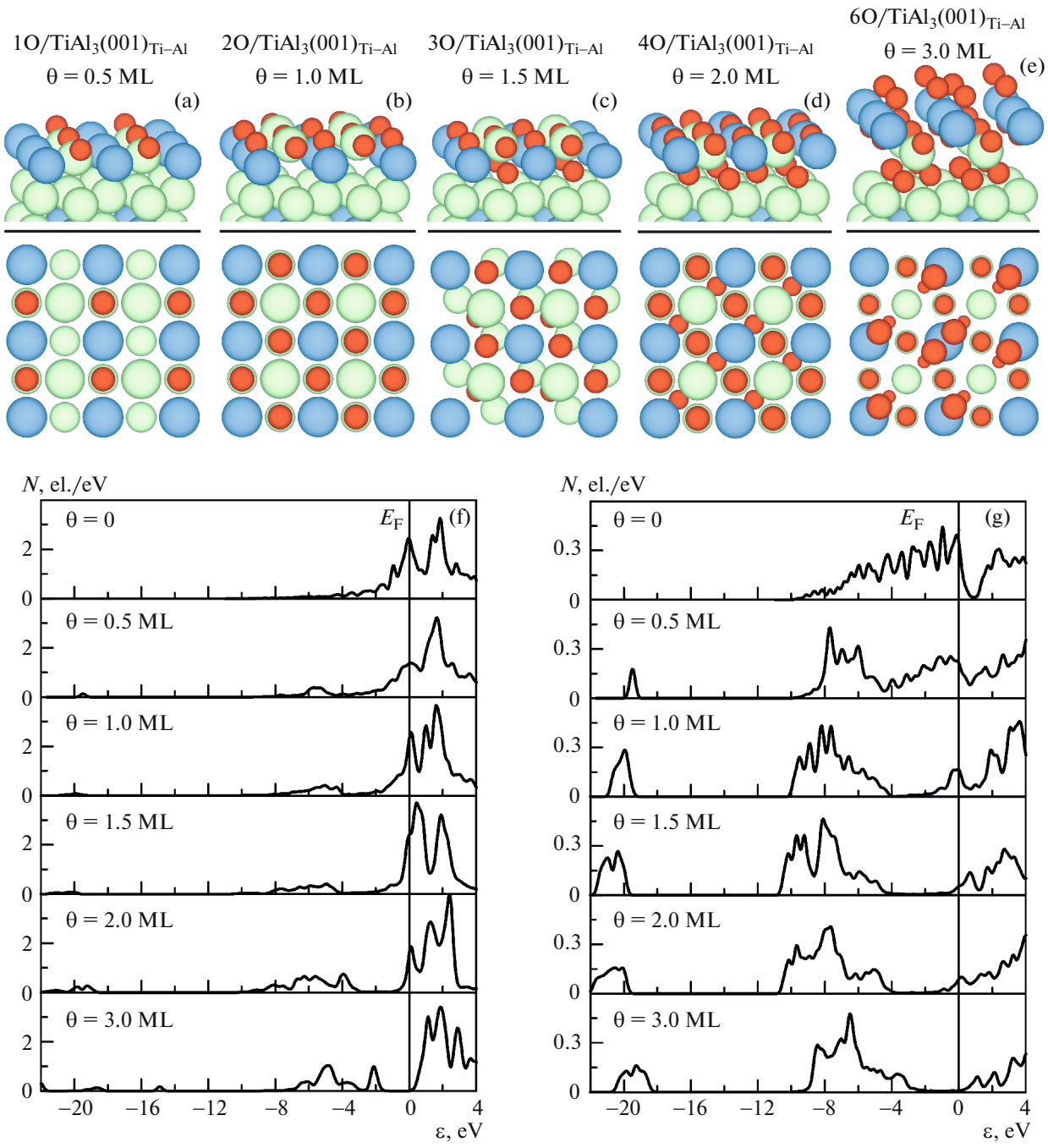

Fig. 9. (Color online) Atomic structures of $TiAl_3(001)_{Ti–Al}$ with a degree of coverage with oxygen from (a–e) 0.5 to 3.0 ML, and the corresponding local DOS of atoms (f) Ti and (g) Al that are nearest to oxygen. The atoms of oxygen, titanium, and aluminum are shown by the red, blue, and light-green balls, respectively.

increase in the size of the computational cell leads to insignificant changes in the values of the barriers (5–10%) and does not affect the established tendencies. Note that the calculations were performed taking into account the relaxation of the positions of the matrix atoms near the position of the oxygen atom for all its configurations, but the symmetry of the lattice in this case was unchanged.

The energy of the absorption of oxygen in the position O2 (Fig. 10) in the center of the octahedron formed by five atoms of aluminum and one atom of titanium is higher by 0.15 eV than in the position O1 in the octahedron formed by four atoms of aluminum and two atoms of titanium. A reverse tendency was obtained in the γ-TiAl alloy, where the absorption of oxygen is more preferred in the octahedron with the

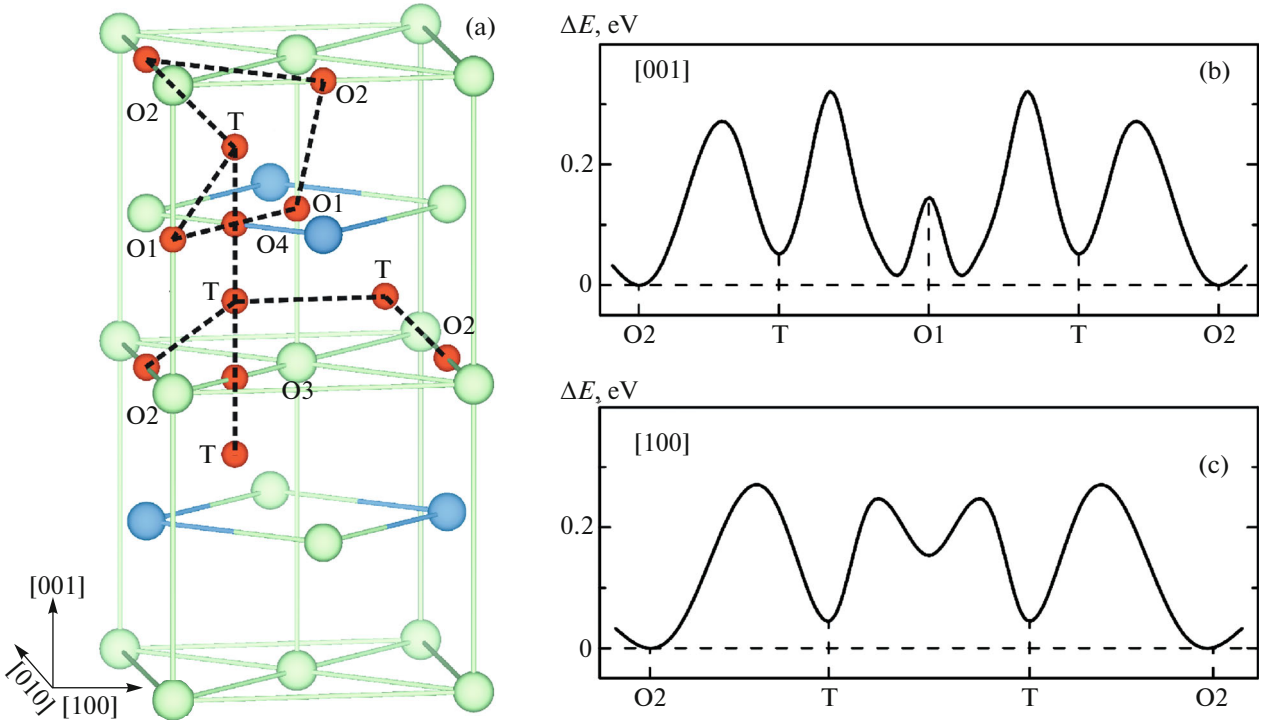

Fig. 10. (Color online) (a) Atomic structure of the unit cell of the $TiAl_3$ alloy with octahedral and tetrahedral positions for the oxygen atom; (b, c) diffusion profiles for the preferable paths of diffusion along the directions (b) [001] and (c) [100].

higher content of titanium. In the $TiAl_3$ alloy, the energy of the absorption of oxygen in the tetrahedron enriched by aluminum, which contains three atoms of aluminum and one atom of titanium, is only 0.05 eV less than in the O2 position. The energy preference of the O2 position for the absorption of oxygen is explained by the same factors that we used earlier for explaining the preference of the bridge B_{TiAl} position on the $TiAl_3(100)$ surface: i.e., by the shift of oxygen toward the titanium and, as a result, by the smaller length of the Ti–O bond than in the O1 position, and also by the larger ionic contribution to the mechanism of chemical bond.

Unlike γ-TiAl [32], in the $TiAl_3$ alloy all positions have in their environment greater number of atoms of aluminum than of titanium. Recall that the diffusion of oxygen in γ-TiAl between the octahedral Ti-rich positions was found to be less preferable than between the Al-rich positions, and on the whole the barriers for the diffusion along the aluminum layers or across these layers were substantially lower than for diffusion from the positions enriched by titanium. This suggests that the barriers for the oxygen diffusion in the alloy enriched by aluminum must be lower than in γ-TiAl.

The calculated values of the energy barriers for the paths shown by dashed lines in Fig. 10a are given in Table 5. It can be seen that the energy barrier between the O2 positions is substantially lower than between the O1 positions with the smaller number of aluminum atoms in the nearest neighbors. Furthermore, the energy barrier between the O1 positions is less approximately by 1.0 eV than between the Ti-rich O1 positions (3.02 eV) in γ-TiAl [32]. The diffusion barrier between the tetrahedral positions along the [001] direction through the O3 position in the aluminum layer (Fig. 10a) is almost four times lower than the corresponding barrier through the O4 position. In the latter case, the saddle point is located in the bridge position between the atoms of aluminum and titanium. It must be noted that although the barrier along the T → O3 → T path is small, it does not correspond to translational diffusion, and it should be considered as part of a more complex way. As follows from Table 5, the energy barriers for oxygen diffusion along the paths O1 → T or O2 → T are also small; in this case, the reverse diffusion T → O2 is more preferable than T → O1, which is caused by the larger preference of the O2 position for the absorption of oxygen. The analysis of the obtained results makes it possible to draw a conclusion that the trajectory with the smallest energy along the direction [001] is O2 → T → O1 → O2 (Fig. 10b); in this case, the activation energy lies in the range of approximately from 0.18 to 0.27 eV.

In the directions [100] and [010], the lowest energy barrier is obtained for the oxygen diffusion over the tetrahedral positions, when it migrates between the aluminum and mixed layers. The barrier for the diffusion of oxygen between the tetrahedral positions is reduced from 0.81 eV in γ-TiAl [32] to 0.18 eV in $TiAl_3$.

Table 5. Values of the energy barriers for the diffusion of oxygen in the $TiAl_3$ alloy

Diffusion path	Height of the barrier, eV
O1 → O1	2.05
O2 → O2	0.58
O2 → O1	1.45
O1 → O2	1.31
O1 → T	0.18
T → O1	0.27
O2 → T	0.25
T → O2	0.20
T → O3 → T	0.52
T → O4 → T	2.14
T → T	0.18

At the same time, the migration of oxygen along the O2 → T → T → O2 trajectory (Fig. 10c) also occurs almost without a barrier. This indicates a high mobility of oxygen in $TiAl_3$ irrespective of the direction of its diffusion.

Thus, the calculations carried out confirmed that with an increase in aluminum concentration the barriers for the diffusion of oxygen between positions enriched by aluminum or through the aluminum layer decrease, just as in the alloy of equiatomic composition. However, the positions near the titanium atoms will not be traps, as in γ-TiAl, since the barriers for diffusion from these positions are sufficiently low. Note that the established tendencies occur also in the titanium-rich Ti_3Al alloy, in which the barriers for diffusion between positions enriched by titanium increase to 3.64 eV. In this work, we do not discuss the results of oxygen diffusion from the surface into the bulk of the alloy, since the tendencies discovered earlier for γ-TiAl [32] remain valid for $TiAl_3$ as well. The formation of a dense protective layer of aluminum oxide will not be suppressed on the surface of $TiAl_3$, since the oxygen atoms are not trapped by the mixed Ti–Al layers in contrast to the titanium layers in TiAl.

4. CONCLUSIONS

Thus, in this work we presented results of the calculations of the adsorption of oxygen on the low-index (001), (100), and (110) surfaces of the $TiAl_3$ alloy, which were performed by the projector augmented-wave method within the framework of the density functional theory. It was shown that on the (001) surface, irrespective of its termination, oxygen prefers to be adsorbed in the H_{Al}-hollow position. On the aluminum termination of the $TiAl_3$(110) surface, which is stable in a wide range of the variation in the chemical potential of aluminum, the energetically preferable for oxygen is the B1 short-bridge position. It was established that the binding energies of oxygen on the mixed terminations of the (001) and (110) surfaces are greater than on the aluminum termination irrespective of the adsorption position. On the stoichiometric $TiAl_3$(100) surface, the largest energy of the oxygen adsorption was obtained for the B_{TiAl} position. An analysis of the structural and electronic factors that are responsible for the energy preference of the positions for oxygen adsorption has been performed.

Changes in the atomic and electronic structure of near-surface layers that occur with an increase in the concentration of oxygen have been analyzed on the example of the (001) surface depending on its termination. The calculations indicate that on the aluminum terminations of the (001) or (110) surfaces, the oxidation of aluminum predominates over the oxidation of titanium, which is in agreement with the experimental data [1, 14, 15] on the oxidation of the surface of the $TiAl_3$ alloy; the process of the formation of the forbidden gap ends at the degree of coverage equal to 2 ML. This reflects the completion of the process of the transformation of the metallic surface into the oxide surface. On the mixed terminations of low-index surfaces, the interaction of oxygen with aluminum prevails over the interaction with titanium at low concentrations (to 1. 5 ML of oxygen), whereas at high concentrations, the bonding of oxygen with titanium is stronger, which leads to the formation of a layer enriched by titanium and, as a result, to the formation of titanium oxides on the surface.

The performed calculation of the energy barriers for the diffusion of oxygen in the $TiAl_3$ alloy has shown that the migration of oxygen is more preferable between the tetrahedral positions both in the region between the aluminum and mixed layer and through the aluminum layer. An increase in the aluminum concentration leads to a reduction in the energy barriers for the oxygen diffusion in the bulk material.

ACKNOWLEDGMENTS

This work was supported in part by the Russian Foundation for Basic Research (project no. 14-02-91150a_GFEN) and by the NSFC (project no. 513111054), and also by the Tomsk State University Competitiveness Improvement Program. The numerical calculations were partially performed using the SKIF-Cyberia supercomputer at the Tomsk State University, and also with the use of resources of the supercomputer complex of the Moscow State University [56].

REFERENCES

1. Z. Li and W. Gao, in *Intermetallics Research Progress,* Ed. by N. Berdovsky (Nova Science, New York, 2008), p. 1.
2. Ya. Polmear, *Light Alloys: From Tradition to Nanocrystals* (Tekhnosfera, Moscow, 2008) [in Russian].

3. F. Motte, C. Coddet, P. Sarrazin, et al., Oxid. Met. **10**, 113 (1976).
4. A. Galerie, Y. Wouters, and J. P. Petit, Mater. Sci. Forum **251–254**, 113 (1997).
5. M. Gobel, J. D. Sunderkotter, D. I. Mircea, et al., Surf. Interf. Anal. **29**, 321 (2000).
6. P. Kofstad, *High Temperature Corrosion* (Elsevier Science, London, 1988).
7. A. Rahmel and P. J. Spencer, Oxid. Met. **35**, 53 (1991).
8. K. L. Luthra, Oxid. Met. **36**, 475 (1991).
9. T. G. Avanesyan, Cand. Sci. (Chem.) Dissertation (Sci.-Res. Tech. Univ. MISiS, Moscow, 2014).
10. S. Becker, A. Rahmel, W. J. Quadakkers, et al., Oxid. Met. **38**, 425 (1992).
11. M. Schmitz-Niederau and M. Schütze, Oxid. Met. **52**, 225 (1999).
12. C. Lang and M. Schütze, Oxid. Met. **46**, 255 (1996).
13. C. Lang and M. Schütze, Mater. Corros. **48**, 13 (1997).
14. Y. Umakoshi, M. Yamaguchi, T. Sakagami, et al., J. Mater. Sci. **24**, 1599 (1989).
15. J. L. Smialek and D. L. Humphrey, Scripta Metall. Mater. **26**, 1763 (1992).
16. K. Hirukawa, H. Mabuchi, and Y. Nakayama, Scripta Metall. Mater. **25**, 1211 (1991).
17. L. J. Parfitt, J. L. Smialek, J. P. Nic, et al., Scripta Metall. Mater. **25**, 727 (1991).
18. S. P. Chen, W. Zhang, Y. H. Zhang, et al., Scripta Metall. Mater. **27**, 455 (1992).
19. D. B. Lee, S. H. Kim, K. Niinobe, et al., Mater. Sci. Eng. A **290**, 1 (2000).
20. N. Yamaguchi, T. Kakeyama, T. Yoshioka, et al., Mater. Trans. JIM **43**, 3211 (2002).
21. C. Woodward, S. Kajihara, and L. H. Yang, Phys. Rev. B **57**, 13459 (1998).
22. Y. Song, R. Yang, D. Li et al., J. Mater. Res. **14**, 2824 (1999).
23. D. Music and J. Schneider, Phys. Rev. B **74**, 174110 (2006).
24. H. Li, M. Liu, S. Q. Wang, et al., Acta Metall. Sinica **42**, 897 (2006).
25. H. Li, S. Wang, and H. Ye, J. Mater. Sci. Technol. **25**, 569 (2009).
26. S. Y. Liu, J. X. Shang, F. H. Wang, et al., Phys. Rev. B **79**, 075419 (2009).
27. H. R. Gong, Y. H. He, and B. Y. Huang, Appl. Phys. Lett. **93**, 101907 (2008).
28. H. R. Gong, Intermetallics **17**, 562 (2009).
29. L. Wang, J. X. Shang, F. H. Wang, et al., J. Phys.: Condens. Matter. **23**, 265009 (2011).
30. Y. Song, J. H. Dai, and R. Yang, Surf. Sci. **606**, 852 (2012).
31. L. Wang, J. Shang, F. H. Wang, et al., Acta Mater. **61**, 1726 (2013).
32. A. V. Bakulin, S. E. Kulkova, Q. M. Hu, and R. Yang, J. Exp. Theor. Phys. **120**, 257 (2015).
33. A. V. Bakulin, S. E. Kulkova, Q. M. Hu, et al., Comput. Mater. Sci. **97**, 55 (2015).
34. T. Hong, T. J. Watson-Yang, and A. J. Freeman, Phys. Rev. B **41**, 12462 (1990).
35. D. G. Pettifor, Mater. Sci. Technol. **8**, 345 (1992).
36. O. I. Velikokhatnyi, S. V. Eremeev, I. I. Naumov, et al., J. Phys.: Condens. Matter **14**, 8763 (2002).
37. Z. Chen, H. Zou, F. Yu, et al., J. Phys. Chem. Sol. **71**, 946 (2010).
38. L. Wang, J. Gong, and J. Gao, Adv. Mater. Res. **299–300**, 417 (2011).
39. P. E. Blöchl, Phys. Rev. B **50**, 17953 (1994).
40. G. Kresse and J. Joubert, Phys. Rev. B: Condens. Matter **59**, 1758 (1999).
41. G. Kresse and J. Hafner, Phys. Rev. B **48**, 13115 (1993).
42. G. Kresse and J. Furthmüller, Phys. Rev. B **54**, 11169 (1996).
43. G. Kresse and J. Furthmüller, Comput. Mater. Sci. **6**, 15 (1996).
44. J. P. Perdew, K. Burke, and M. Ernzerhof, Phys. Rev. Lett. **77**, 3865 (1996).
45. H. J. Monkhorst and J. D. Pack, Phys. Rev. B **13**, 5188 (1976).
46. P. Norby and A. N. Christensen, Acta Chem. Scand. A **40**, 157 (1986).
47. H. Shi and C. Stampfl, Phys. Rev. B **76**, 075327 (2007).
48. K. P. Huber and G. Herzberg, *Molecular Spectra and Molecular Structure IV: Constants of Diatomic Molecules* (Van Nostrand Reinhold, New York, 1979).
49. G. Mills, H. Jónsson, and G. K. Schenter, Surf. Sci. **324**, 305 (1995).
50. G. Henkelman, B. P. Uberuaga, and H. Jónsson, J. Chem. Phys. **113**, 9901 (2000).
51. O. J. Kleppa, J. Phase Equilibr. **15**, 240 (1994).
52. R. Hultgren, P. D. Desai, D. T. Hawkins, et al., *Selected Values of the Thermodynamic Properties of Binary Alloys* (Amer. Society for Metals, Ohio, 1973).
53. M. R. Shanabarger, Appl. Surf. Sci. **134**, 179 (1998).
54. M. Ramachandran, D. Mantha, C. Williams et al., Metall. Mater. Trans. A **42**, 202 (2011).
55. F. P. Ping, Q. M. Hu, A. V. Bakulin, et al., Intermetallics **68**, 57 (2016).
56. V. Voevodin, S. Zhumatii, S. Sobolev, et al., Otkryt. Sist. **7**, 36 (2012).

Translated by S. Gorin